Supplementary Information

$[Cd_4P_2][I_3]$ and $[Cd_2P][CdCl_3]$: Two Millon's phase phosphides exhibiting wide band gaps and large birefringence

Abstract: Research on infrared birefringent crystals applicable to the 8-12 μm long-wave infrared region remains extremely scarce to date. Herein, two Millon's phase phosphides infrared birefringent crystals $[Cd_4P_2][I_3]$ and $[Cd_2P][CdCl_3]$, are reported. Both $[Cd_4P_2][I_3]$ and $[Cd_2P][CdCl_3]$ exhibit a large birefringence (0.105, 0.139) at 546 nm, and good IR transparency (up to 15 μm) and wide band gap (2.20, 2.72 eV). The P-P covalent bonds in $[Cd_4P_2][I_3]$ effectively enhance the structural anisotropy of this phosphide, which constitutes the intrinsic origin of its large birefringence. The chain-layer interconnected arrangement within $[Cd_2P][CdCl_3]$ is responsible for the pronounced structural anisotropy of the crystal, a critical structural factor giving rise to its large birefringence. These results demonstrate the great potential of $[Cd_4P_2][I_3]$ and $[Cd_2P][CdCl_3]$ with "Millon's phase" structure as birefringent materials for applications in the long-wave infrared region.

Table of Contents

Experimental Section

Materials and syntheses.

The raw materials were Cd_3P_2 (3N, Aladdin) and CdI_2/$CdCl_2$ (3N, Adamas), which were not further purified. The mixture of Cd_3P_2 and CdI_2 at a 1:5 molar ratio was loaded into a vacuum-sealed quartz tube and the mixture of Cd_3P_2 and $CdCl_2$ at a 1:3 molar ratio was loaded into a vacuum-sealed quartz tube. The Cd_3P_2 and CdI_2 were placed into a muffle furnace, heated to 700 °C, holding for 3 days, and slowly cooled to 300 at rate of 3 °C /h before naturally cooling. The Cd_3P_2 and $CdCl_2$ were placed into a muffle furnace, heated to 500 °C, holding for 3 days, and slowly cooled to 300 at rate of 3 °C /h before naturally cooling. The products contained orange- red $[Cd_4P_2][I_3]$ and $[Cd_2P][CdCl_3]$ bulk crystals were physically separated out, and then were washed using ethyl alcohol to remove remained CdI_2 and $CdCl_2$. All the title compounds and byproducts were air- and moisture-stable.

Single-Crystal X-Ray Diffraction.

The diffraction data were collected at room temperature on a Bruker SMART APEX III 4K CCD diffractometer and Mo Kα radiation (λ = 0.71073 Å) at 296(2) K.[1] The data was integrated by SHELXL-2018/3, and the multi-scan method was used to the absorption corrections. The crystal structure of the two compounds was determined by the intrinsic phasing methods and refined with anisotropic thermal parameters for all atoms by full-matrix leasts-quares fitting on F^2 using SHELXL on Olex2 program.[2-3] The PLATON program[4] was used to check the correctness of the structures, and no higher symmetries were found. The crystal data and structure refinement parameters were shown in Table S1. Some structural parameters including interatomic distances, final refined atomic positions and anisotropic displacement parameters are listed in Table S2, Table S3, and Table 4, respectively.

Birefringence measurements.

Due to the existence of birefringence in anisotropic crystals, linearly polarized light is divided into two beams (ordinary light and extraordinary light) along the optical principal axis of its luminous volume cross section as it passes through the crystal. These two lights have different speed resulting retardation. In the cross-polarizing system, the two beams of polarizing light passing through the polarizer satisfy the interference condition, so they can superimpose and interfere with each other to show the interference color. This interference color is determined by the magnitude of the light path difference. By using cross-polarizing microscope, their birefringence was evaluated based on the formula $R = \Delta n \times d$, where R, d, and Δn are retardation, the thickness of the measured flat transparent massive crystal, and birefringence.[5] The experimental result showed that the interference color of cross polarized light was the second order orange and the third order green, the value of R of $[Cd_4P_2][I_3]$ is 960 nm and d is 9.5 μm for $[Cd_4P_2][I_3]$. The birefringence of $[Cd_4P_2][I_3]$ is about 0.101 in the visible region. The value of R of $[Cd_2P][CdCl_3]$ is 1250nm and d is 9.2 μm for $[Cd_2P][CdCl_3]$. The birefringence of $[Cd_2P][CdCl_3]$ is about 0.136 in the visible region.

Powder X-Ray Diffraction.

The Powder X-ray diffraction (XRD) patterns data of $[Cd_4P_2][I_3]$ and $[Cd_2P][CdCl_3]$ were collected from 10° to 70° (2θ) with a step width size of 0.01° and a step time of 2s on a SmartLab9KW powder X-ray diffractometer with Cu-Kα radiation.

Elemental Analysis.

The element content of Cd and P and I was accurately identified by inductively a field emission scanning electron microscope (Quanta FEG 250) equipped with an energy-dispersive X-ray spectrometer, which is listed in FigureS2.

UV-Vis-NIR diffuse reflectance spectrum.

The Shimadzu SolidSpec-3700DUV spectrophotometer was employed to measure UV-vis-NIR diffuse reflectance spectrum of $[Cd_4P_2][I_3]$ and $[Cd_2P][CdCl_3]$ in a wavelength range from 240 nm to 2400 nm at room temperature.

$BaSO_4$ was selected as the standard for 100% reflectance comparison. The reflectance value is converted to absorbance by using the Kubelka-Munk function.[6-7]

Microscopic infrared transmission spectroscopy.

Microscopic infrared transmission spectroscopy was conducted using a Nicolet iN10 instrument on crystal wafers visible to the naked eye, approximately 1mm in size. The wavenumber range of the microscopic infrared transmission spectrometer is only capable of testing from 675-4000 cm^{-1}. The tested crystal wafers must be of good quality, flat, and free of cracks. The wavelength test range for the two crystal examples, $[Cd_4P_2][I_3]$ and $[Cd_2P][CdCl_3]$, is 2.5-14.8 μm. Since they do not reach the infrared cut-off edge at 14.8 μm, the wavelength range for both crystal examples is greater than 15 μm.

Raman Spectroscopy.

The Raman spectra of the compounds were obtained by a confocal microscope laser Raman spectrometer (inVia Qontor) equipped with a CCD detector. The radiation wavelength of $[Cd_4P_2][I_3]$ and $[Cd_2P][CdCl_3]$ single crystals was 785nm, the laser intensity was 5%.

Theoretical Calculation Details.

The electronic structure calculations were performed by the first-principles calculations in the CASTEP package, [8-9] with the Norm-conserving pseudopotentials. [10] The Perdew-Burke-Ernzerhof (PBE) functional [11] within the generalized gradient approximation (GGA) was applied for the exchange-correlation potential. [12] The following orbital electrons were treated as valence electrons, Cd: $4d^{10}5s^25p^0$, P: $3s^23p^3$, I: $5s^25p^5$, Cl: $3s^23p^5$. To achieve energy convergence, the plane-wave energy cutoff was set at 720 eV. The Brillouin zone involved 4 × 4 × 4. As important parameters for NLO crystals, the birefringence was also calculated with suitable scissor operators.

Results and Discussion

Table S1. Crystal data and structure refinement for $[Cd_4P_2][I_3]$ and $[Cd_2P][CdCl_3]$

Empirical formula	**$[Cd_4P_2][I_3]$**	**$[Cd_2P][CdCl_3]$**
Formular weight	892.24	474.52
Temperature (K)	273(2)	273(2)
Radiation	MoKα (λ = 0.71073)	MoKα (λ = 0.71073)
Space group	*Pbca*	*Pnma*
a (Å)	12.7104(4)	13.0291(6)
b (Å)	12.6393(3)	7.9646(4)
c (Å)	12.8670(4)	7.0077(3)
Volume ($Å^3$)	2067.09(10)	727.20(6)
Z	8	4
$\rho calc$ (mg/m^3)	5.734	4.334
μ (mm^{-1})	17.311	9.892
F (000)	3048	840
Index ranges	$-16 \leq h \leq 16$, $-16 \leq k \leq 16$, $-16 \leq l \leq 16$	$-14 \leq h \leq 16$, $-10 \leq k \leq 10$, $-9 \leq l \leq 8$
Reflections collected/unique	16409/2382 [$R_{int} = 0.0571$]	4467/866 [$R_{int} = 0.0467$]
Data/restraints/parameters	2382/0/86	866/0/41
Final *R* indexes [I>=2σ (I)]	$R_1 = 0.0320$, $wR_2 = 0.0766$	$R_1 = 0.0237$, $wR_2 = 0.0481$
Final R indexes [all data]	$R_1 = 0.0359$, $wR_2 = 0.0784$	$R_1 = 0.0315$, $wR_2 = 0.0512$
Largest diff. peak/hole (e $Å^{-3}$)	3.09/-2.11 $eÅ^{-3}$	0.708/-0.646 $eÅ^{-3}$
Goodness-of-fit on F^2	1.137	1.095

[a] $R_1 = F_o - F_c / F_o$ and $wR_2 = [w(F_o^2 - F_c^2)^2 / wF_o^4]^{1/2}$ for $F_o^2 > 2\sigma(F_o^2)$

Table S2. Atomic Coordinates ($\times 10^4$) and Equivalent Isotropic Displacement Parameters ($Å^2 \times 10^3$).

	x	**y**	**z**	**U(eq)**
		$[Cd_4P_2][I_3]$		
Cd(1)	4264(1)	5411(1)	2148(1)	39(1)
Cd(2)	5696(1)	5945(1)	5178(1)	29(1)
Cd(3)	2902(1)	4121(1)	-579(1)	33(1)
Cd(4)	5742(1)	2967(1)	929(1)	29(1)
P(1)	4516(2)	4469(1)	473(1)	12(1)
P(2)	4021(2)	5965(1)	3982(1)	13(1)
I(1)	6763(1)	4369(1)	2484(1)	20(1)
I(2)	5705(1)	7471(1)	6812(1)	21(1)
I(3)	7528(1)	6827(1)	4251(1)	20(1)
		$[Cd_2P][CdCl_3]$		
Cd(1)	7528(1)	7500	-37(1)	27(1)
Cd(2)	5000	5000	0	29(1)

Cd(3)	5865(1)	7500	4848(1)	28(1)
P(1)	5796(1)	7500	1376(2)	16(1)
Cl(1)	9177(1)	7500	-1901(2)	25(1)
Cl(2)	6702(1)	9783(1)	6902(1)	27(1)

Table S3. Selected Bond Lengths and Angles for [Cd$_4$P$_2$][I$_3$]and [Cd$_2$P][CdCl$_3$].

[Cd$_4$P$_2$][I$_3$]		**[Cd$_2$P][CdCl$_3$]**	
Cd(1)-P(2)	2.4831(19)	Cd(1)-P(1)	2.4645(13)
Cd(1)-P(2)	2.4810(19)	Cd(2)-P(1)	2.4432(7)
Cd(2)-P(2)	2.626(2)	Cd(2)-P(1)$^{\#3}$	2.4431(7)
Cd(2)-P(2)$^{\#6}$	2.6694(19)	Cd(3)-P(1)	2.4349(13)
Cd(3)-P(1)	2.497(2)	Cd(1)-Cl(1)	2.5155(13)
Cd(3)-P(2)$^{\#7}$	2.511(2)	Cd(3)-Cl(1)$^{\#5}$	2.6270(14)
Cd(1)-I(2)$^{\#2}$	3.2717(10)	Cd(1)-Cl(2)$^{\#1}$	2.7454(9)
Cd(1)-I(3)$^{\#3}$	3.3639(10)	Cd(1)-Cl(2)$^{\#2}$	2.7454(9)
Cd(3)$^{\#1}$-I(1)	3.1359(9)	Cd(3)-Cl(2)	2.5623(10)
Cd(4)-I(1)	2.9705(8)	Cd(3)-Cl(2)$^{\#4}$	2.5623(10)
P(1)-P(1)$^{\#1}$	2.190(4)	P(1)-Cd(1)-Cl(1)	172.40(5)
P(1)-Cd(1)-I(2)$^{\#2}$	101.87(5)	P(1)-Cd(1)-Cl(2)$^{\#1}$	97.82(3)
P(1)-Cd(1)-I(3)$^{\#3}$	82.84(5)	P(1)-Cd(1)-Cl(2)$^{\#2}$	97.82(3)
P(1)-Cd(3)-I(1)$^{\#1}$	101.82(5)	P(1)-Cd(3)-Cl(1)$^{\#5}$	121.08(4)
P(1)-Cd(4)-I(1)	88.71(5)	P(1)-Cd(3)-Cl(2)	125.23(3)
P(1)-Cd(4)-I(3)$^{\#12}$	102.31(5)	P(1)-Cd(3)-Cl(2)$^{\#4}$	125.24(3)
P(2)-Cd(1)-I(2)$^{\#2}$	87.96(5)	P(1)-Cd(2)-P(1)$^{\#3}$	180.0
P(2)-Cd(1)-I(3)$^{\#3}$	106.09(5)	Cl(1)-Cd(1)-Cl(2)$^{\#1}$	86.82(3)
P(2)-Cd(2)-I(2)	115.35(5)	Cl(1)-Cd(1)-Cl(2)$^{\#2}$	86.82(3)
P(2)$^{\#6}$-Cd(2)-I(2)	108.19(5)	Cl(2)$^{\#2}$-Cd(1)-Cl(2)$^{\#1}$	104.06(4)
P(2)-Cd(2)-I(3)	114.48(5)	Cl(2)-Cd(3)-Cl(2)$^{\#5}$	92.80(3)
P(2)$^{\#6}$-Cd(2)-I(3)	114.46(5)	Cl(2)$^{\#4}$-Cd(3)-Cl(2)$^{\#5}$	92.80(3)
P(2)$^{\#7}$-Cd(3)-I(1)$^{\#1}$	89.02(5)	Cl(2)-Cd(3)-Cl(2)$^{\#4}$	90.39(4)
P(2)$^{\#7}$-Cd(3)-I(2)$^{\#10}$	113.81(5)		
P(2)$^{\#10}$-Cd(4)-I(1)	120.67(5)		
P(2)$^{\#10}$-Cd(4)-I(3)$^{\#12}$	91.77(5)		
P(1)-Cd(1)-P(2)	167.69(7)		
P(1)-Cd(3)-P(2)$^{\#7}$	158.33(7)		
P(1)-Cd(4)-P(2)$^{\#10}$	145.99(7)		
P(2)-Cd(2)-P(2)$^{\#6}$	110.83(5)		
I(1)$^{\#1}$-Cd(3)-I(2)$^{\#10}$	86.17(2)		
I(1)-Cd(4)-I(3)$^{\#12}$	96.30(2)		
I(3)$^{\#3}$-Cd(1)-I(2)$^{\#2}$	82.03(2)		
I(3)-Cd(2)-I(2)	92.31(2)		

Symmetry transformations used to generate equivalent atoms: #1-x+3/2,y-1/2,z-1/2 #2-x+3/2,-y+2,z-1/2 #3 -x+1,-y+1,-z #4 x-1/2,y,-z+1/2 #5 x,-y+3/2,z #6 x+1/2,y,-z+1/2 #7 -x+3/2,-

y+2,z+1/2 #8 -x+1,y+1/2,-z

Table S4. Anisotropic Displacement Parameters (Å^2×10^3) for [Cd_4P_2][I_3] and [Cd_2P][$CdCl_3$].

Atom	U_{11}	U_{22}	U_{33}	U_{23}	U_{13}	U_{12}
			[Cd_4P_2][I_3]			
Cd(1)	61(1)	39(1)	17(1)	-10(1)	9(1)	2(1)
Cd(2)	29(1)	21(1)	36(1)	4(1)	-11(1)	-6(1)
Cd(3)	17(1)	36(1)	45(1)	-2(1)	-12(1)	-3(1)
Cd(4)	34(1)	14(1)	39(1)	1(1)	-5(1)	6(1)
P(1)	12(1)	13(1)	13(1)	1(1)	0(1)	1(1)
P(2)	14(1)	13(1)	12(1)	-2(1)	2(1)	0(1)
I(1)	19(1)	21(1)	20(1)	1(1)	-3(1)	-3(1)
I(2)	24(1)	19(1)	19(1)	0(1)	3(1)	0(1)
I(3)	18(1)	20(1)	21(1)	-3(1)	-1(1)	0(1)
			[Cd_2P][$CdCl_3$]			
Cd(1)	19(1)	33(1)	30(1)	0	6(1)	0
Cd(2)	33(1)	21(1)	35(1)	-5(1)	-5(1)	-8(1)
Cd(3)	33(1)	34(1)	17(1)	0	-1(1)	0
P(1)	16(1)	15(1)	16(1)	0	0(1)	0
Cl(1)	19(1)	34(1)	22(1)	0	4(1)	0
Cl(2)	32(1)	25(1)	23(1)	3(1)	-1(1)	-8(1)

Table S5. The band gap and birefringence of P-P-containing pnictides.

Pnictides	E_g (eV)	Birefringence
[Cd_4P_2][I_3]	2.52 eV	0.105@546 nm
α/β-Cd_2P_3Cl	/	0.24/0.29@1064 nm
α/β-Cd_2P_3Br	/	0.19/0.18@1064 nm
α/β-Cd_2P_3I	/	0.04/0.03@1064 nm
α-CdP_2	2.01 eV	0.138@2050 nm
β-CdP_2	1.98 eV	0.048@2050 nm
$SrIn_3Si_4P_{11}$	1.67 eV	0.10@1910 nm

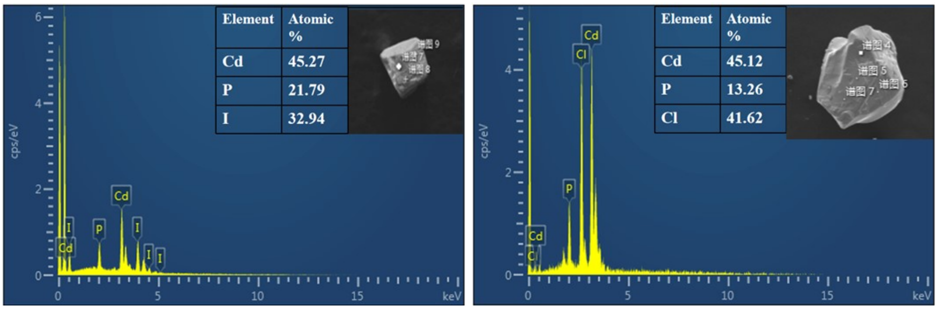

Element	Atomic %
Cd	45.27
P	21.79
I	32.94

Element	Atomic %
Cd	45.12
P	13.26
Cl	41.62

Figure S1. Energy-dispersive X-ray spectroscopy analysis of [Cd_4P_2][I_3] and [Cd_2P][$CdCl_3$].

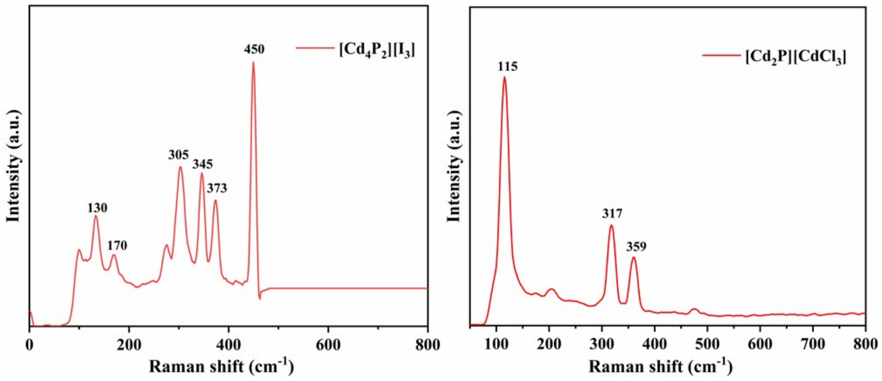

Figure S2. Raman scattering spectra of [Cd_4P_2][I_3] and [Cd_2P][$CdCl_3$].

Reference:

[1] R. Masse, J.C. Grenier, A. Durif-Varambon, et al., Minéralogie. 90 (1967) 20-23.

[2] G. M. Sheldrick, Acta. Crystallogr. C. 71(2015) 3-8.

[3] G. M. Sheldrick, Acta. Crystallogr. Sect. A: Found. 64 (2008) 112-122.

[4] A. Spek, J. Appl. crystallogr. 36 (2003) 7-13.

[5] J. P. Perdew, K. Burke, M. Ernzerhof, Phys. Rev. Lett. 77 (1996) 3865.

[6] P. Kubelka, F. Munk, Z. Tech. Phys. 12 (1931) 259-274.

[7] J. Tauc, Mater. Res. Bull. 5 (1970) 721-729.

[8] W. Kohn, L. J. Sham, Phys. Rev. 140 (1965) A1133-A1138.

[9] G. Sheldrick, Acta. Crystallogr. Sect. 64 (2008) 112-122.

[10] S. J. Clark, M. D. Segall, C. J. Pickard, et al., Z. Krist-Cryst. Mater. 220 (2005) 567-570.

[11] J. P. Perdew, Y. Wang, Phys. Rev. B. 46 (1992) 12947-12954.

[12] J. P. Perdew, A. Ruzsinszky, G. I. Csonka, et al., Phys. Rev. Lett. 100 (2008) 136406.